Citation: Steiner, A.K., A. Löscher, and G. Kirchengast: Error Characteristics of Refractivity Profiles Retrieved from CHAMP Radio Occultation Data, in: Atmosphere and Climate: Studies by Occultation Methods (U. Foelsche, G. Kirchengast, A.K. Steiner, eds.), Springer, Berlin-Heidelberg, 27-36, 2006.

Error Characteristics of Refractivity Profiles Retrieved from CHAMP Radio Occultation Data

A. K. Steiner, A. Löscher, and G. Kirchengast

Wegener Center for Climate and Global Change (WegCenter) and Institute for Geophysics, Astrophysics, and Meteorology (IGAM), University of Graz, Austria
andi.steiner@uni-graz.at

Abstract. We present results of an empirical error analysis of refractivity profiles based on CHAMP radio occultation data. We analyzed two seasons of observations, boreal winter 2002/03 and boreal summer 2003. The processing was performed with the WegCenter/CHAMPCLIM Retrieval version 2. The error statistics is based on comparison to reference profiles calculated from ECMWF analyses fields. Bias profiles and error covariance matrices are provided, the latter separated into standard deviation profiles and error correlation matrices. Since the error characteristics contain both the observational error of the retrieved data and the model error of the ECMWF analyses we performed an estimation of the ECMWF model error and separated the observation error. The relative refractivity bias of CHAMP radio occultation data with respect to ECMWF was found to oscillate around –0.4 % at 5–25 km globally. Wavelike structures apparent at high latitudes in Southern Hemisphere winter are mainly due to the representation of the polar vortex in the ECMWF analyses. The combined relative standard deviation was found to be 0.7–1 % at 5–25 km height globally, showing larger values in winter than in summer in the upper stratosphere at mid- and high latitudes. The global observation error for CHAMP refractivity was estimated to be 0.5–0.75 % at 6–30 km. The results are compared to the findings of Kuo et al. (2004) and to those of an end-to-end simulation study being the precursor of this work (Steiner and Kirchengast 2004, 2005). Based on the simulation study we provide simple observation error covariance matrix formulations for CHAMP refractivity for convenient use in retrieval algorithms and in data assimilation systems.

1 Introduction

The assimilation of radio occultation (RO) data has the potential to significantly improve the accuracy of global and regional meteorological analysis and weather prediction, which has been confirmed by several studies (e.g., Kuo et al. 2000; Healy et al. 2005). One important issue in this respect is knowledge of radio occultation measurement errors in order to formulate adequate observation error covariance matrices for data assimilation systems.

Since refractivity seems to be the most appropriate parameter for assimilation purposes (Syndergaard et al. 2006; Healy et al. 2005) we performed an empirical error analysis of a set of refractivity profiles retrieved from CHAMP RO observations. Regarding the error analysis method, we build on the heritage of an earlier simulation study (Steiner and Kirchengast 2004, 2005) and extend it to a separate estimation of the observation error for CHAMP refractivity data.

Section 2 gives a brief description of the data set and the retrieval algorithms. In Sect. 3 the estimation of the combined error (CHAMP RO plus ECMWF) is described. The ECMWF model error is estimated in Sect. 4 and the results on the observed refractivity error are presented in Sect. 5. Summary and conclusions are drawn in Sect. 6.

2 Description of the Data Set and the Retrieval Scheme

The study is based on a CHAMP level 2 data set comprising two seasons of radio occultation observations, DJF 2002/2003 (December-January-February) and JJA 2003 (June-July-August). For each season more than 12 000 profiles of atmospheric excess phases were analyzed. The data sets were separated into three latitude bands, low (−30° to +30°), middle (±30° to ±60°), and high (±60° to ±90°) latitudes. In addition, we separately analyzed the Northern Hemispheric (NH) and the Southern Hemispheric (SH) region. The sample sizes for the various analyzed data sets are listed in Table 1. Refractivity profiles were processed from this data base of excess phase profiles with the CHAMPCLIM Retrieval version 2 (CCRv2), which includes an advanced upper stratospheric retrieval scheme (Gobiet and Kirchengast 2004a, 2004b). The retrieval is based on the standard geometric optics approach, thus we will not interpret the results below 5 km height. For the upper-boundary initialization of bending angles we used the MSISE-90 climatological model. The CCRv2 processing is described in detail by Steiner et al. (2004) and an overview is included in Borsche et al. (2006).

Table 1. The number of occultation events for the different data sets analyzed.

	DJF 2002/2003			**JJA 2003**		
	Total	***NH***	***SH***	***Total***	***NH***	***SH***
Global	**12329**	5995	6334	**12710**	5989	6721
Low lat	3790	1812	1978	3784	1841	1943
Mid lat	4310	2120	2190	4095	1983	2112
High lat	4229	2063	2166	4831	2165	2666

3 Estimation of the Combined Error

The error statistics is based on the comparison of the retrieved and smoothed (comparable to ECMWF vertical grid resolution) refractivity profiles with co-located refractivity profiles derived from 6-hourly operational meteorological analyses fields from ECMWF. The co-located vertical ECMWF profiles were calculated at a fixed mean tangent point location. When regarding the ECMWF profiles as the truth this implies that the error estimates represent an upper bound error estimate including the observation error, the model (ECMWF) error and the representativeness error. The representativeness error stems from the limited spatial and temporal measurement resolution and from the comparison of the retrieved profiles with vertical reference profiles. The latter fact is important in the troposphere below ~7 km, where higher horizontal variability is present (Foelsche and Kirchengast 2004; Syndergaard et al. 2004). Since we will not interpret results below 5 km, the representativeness errors to this end are largely negligible.

The statistical method for calculating the deviation of CHAMP from ECMWF ($x_{CHAMP} - x_{ECMWF}$), denoted as combined error (CHAMP observed error plus ECMWF model error), is described in detail in Steiner and Kirchengast (2004). Bias profiles and error covariance matrices are provided, the latter separated into standard deviation profiles and error correlation matrices.

The resulting error statistics for the combined refractivity error is shown in Fig. 1 for the global ensemble and the latitudinal data sets (horizontal panel rows), globally (left), for the Northern Hemisphere (middle), and the Southern Hemisphere (right) up to 35 km height. The relative bias (gray) and the relative standard deviation (Rel.StdDev) (black) of CHAMP RO with respect to ECMWF are shown for the JJA 2003 season (solid) and for the DJF 2002/2003 season (dashed).

The refractivity bias of CHAMP RO with respect to ECMWF oscillates around –0.4 % at 5–25 km globally as well as at mid- and high latitudes, increasing to 0.5–1 % at 35 km. Bias oscillations are seen at low latitudes, ranging from –0.4 % to 0.5 % at 5–35 km, with salient structures appearing at tropopause heights. This effect may partly be due to the higher resolved tropopause in CHAMP RO data than in ECMWF data (RO resolution ~1 km at that altitude, ECMWF analyses >1.3 km) but may also stem from a weak representation of tropopause height variability in ECMWF (Gobiet et al. 2005). The most prominent features can be seen in SH winter at high latitudes (lower left panel), which is an indication that the ECMWF field does not accurately represent the polar vortex in this region (Gobiet et al. 2005). The smallest bias occurs at NH high latitudes (lower middle panel) being about –0.3 % at 5–25 km in DJF almost vanishing in JJA.

The combined Rel.StdDev is of the order of 0.7–1 % at 5–28 km height globally and at low latitudes (NH and SH). At mid- and high latitudes the Rel.StdDev shows different behavior in the winter hemisphere and in the summer hemisphere at upper stratospheric heights, being 0.75–1 % at 20–34 km in summer becoming twice as large (~2 % at 35 km) in winter. This may partly be due to the larger atmospheric variability in winter and is subject to further investigation.

4 Estimation of the ECMWF Error

In order to separate the observed error of the CHAMP RO refractivity retrievals from the combined error, we calculated a global estimate of the ECMWF refractivity model error. M. Fisher (ECMWF Reading, UK, pers. communications, 2004) provided global error estimates of ECMWF analyses in form of standard deviations for temperature, specific humidity, and surface pressure, and of vertical error correlations for temperature and specific humidity. Temperature T (K), water

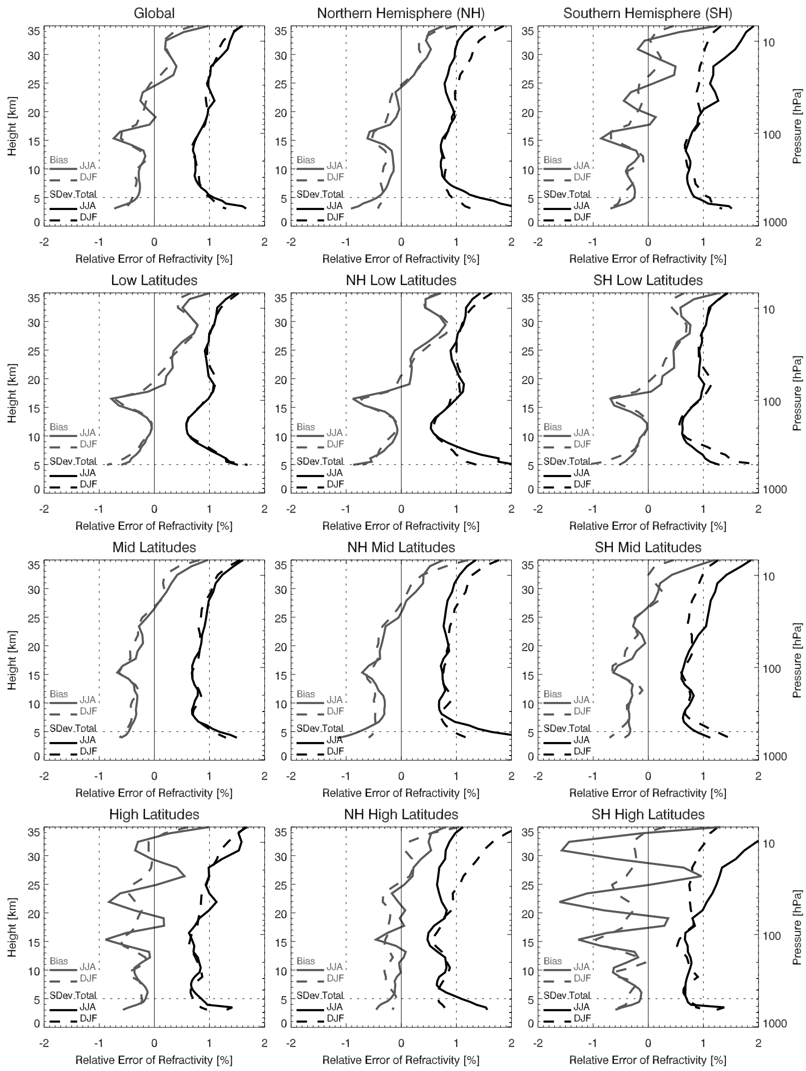

Fig. 1. Combined refractivity error as a function of height for the global and the latitudinal ensembles (horizontal panel rows), globally (left), Northern Hemisphere (middle), Southern Hemisphere (right). Relative bias (gray) and relative standard deviation (black) are shown for the JJA 2003 season (solid) and for the DJF 2002/03 season (dashed), respectively.

vapor pressure e (hPa), and total pressure p (hPa) are related to refractivity N (N units) via the Smith-Weintraub formula (Smith and Weintraub 1953),

$$N = c_1 \frac{p}{T} + c_2 \frac{e}{T^2}, \tag{1}$$

with the constants $c_1 = 77.6$ K/hPa and $c_2 = 3.73 * 10^5$ K^2/hPa. Water vapor pressure in Eq. 1 was substituted for specific humidity q (kg/kg) using the following relation,

$$e = \frac{p \cdot q}{a + bq}, \tag{2}$$

with a = 0.622 and b = 0.378. A simple error propagation based on Eq. 1 was applied via

$$\Delta N = \sqrt{\left(\frac{\partial N}{\partial T}\Delta T\right)^2 + \left(\frac{\partial N}{\partial q}\Delta q\right)^2 + \left(\frac{\partial N}{\partial p}\Delta p\right)^2}, \tag{3}$$

in order to calculate the standard deviation of refractivity. The pressure error at a given height was calculated by error propagation using the given standard deviation of surface pressure of 2.5 hPa. The vertical refractivity error correlations were derived by a weighted combination of temperature error correlations ($w_T = \Delta N(\Delta p,\Delta T)/\Delta N(\Delta p,\Delta q,\Delta T)$) and specific humidity error correlations ($w_q = \Delta N(\Delta q)/\Delta N(\Delta p,\Delta q,\Delta T)$).

Figure 2 displays global ECMWF error specifications for temperature (left panels), specific humidity (middle panels), and estimated refractivity (right panels). Standard deviations are shown in the upper panel row and error correlation functions for three different height levels (~10 km, ~20 km, ~30 km for T and N; ~3 km, ~6 km, ~10 km for q) are presented in the lower panel row.

We tested the sensitivity of the estimated refractivity error with respect to the temperature error input for the four cases displayed in Fig. 2, where we multiplied the temperature standard deviation (case 1xT in light gray) by 1.5 (middle gray), 2 (dark gray), and 2.5 (black). The results judged most reasonable were found for the case of doubling the temperature standard deviation (2xT case), giving a Rel.StdDev of ECMWF refractivity of the order of 0.5 % at 8–15 km increasing to 0.75 % at 30 km and to 1 % at 35 km. These results are consistent with the findings of Kuo et al. (2004) who performed an estimation of short-range forecast errors using the Hollingsworth-Lönnberg method (Hollingsworth and Lönnberg 1986). For comparison we included their estimates for low latitudes (dotted) and mid-latitudes (dashed) in Fig. 2 (upper right panel).

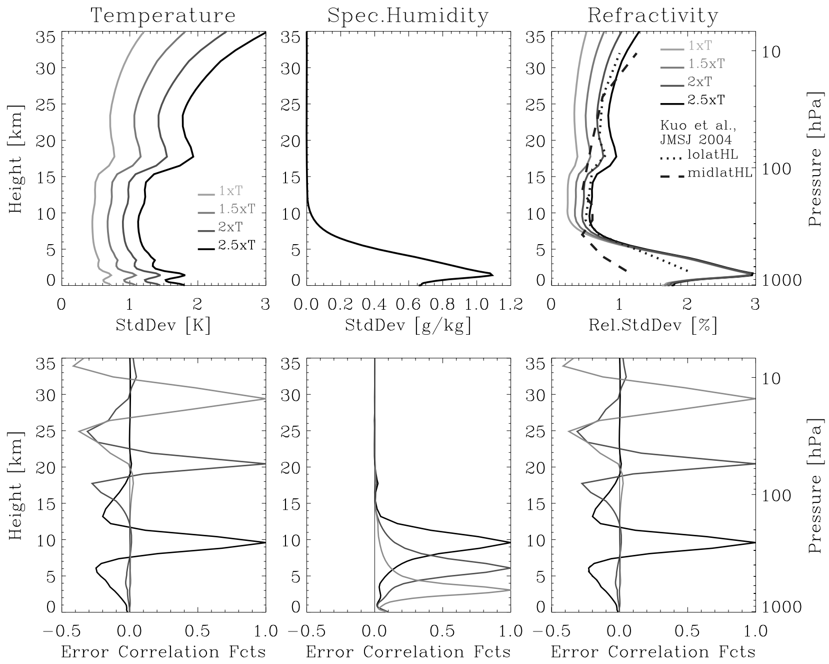

Fig. 2. ECMWF error for temperature (left) for 4 test cases (1x*T*, 1.5x*T*, 2x*T*, 2.5x*T*), specific humidity (middle), and corresponding estimated refractivity (right) in terms of standard deviation (upper panels) and error correlation functions (lower panels), the latter shown for three heights (~10 km (black), ~20 km/humidity: 6 km (gray), ~30 km/humidity: 3 km (light gray)). Estimates of short-range forecast errors for refractivity for low latitudes (dotted) and mid-latitudes (dashed) made by Kuo et al. (2004) are also shown (upper right panel).

5 Estimation of the Observation Error

The observed refractivity error was then derived by subtracting the ECMWF error from the combined error in terms of variances s^2,

$$(s_{\text{obs}})^2 = (s_{\text{combined}})^2 - (s_{\text{ECMWF}})^2 . \tag{4}$$

The results are displayed in Fig. 3 for the JJA season showing the combined error (black with diamond symbols), the ECMWF error for the 2x*T* case (gray), and the corresponding observation error (black) in terms of Rel.StdDev, respectively.

The corresponding global estimate of the observed Rel.StdDev for CHAMP refractivity (2x*T* case) is of the order of 0.5 % at 6–18 km, increasing to 0.7 % at

28 km and to 1.2 % at 35 km (left panel). At upper stratospheric heights the observed Rel.StdDev is around 0.5 % at 10–32 km in summer (middle panel) whilst it reaches 1–1.5 % in winter. Our observation error appears to be a more conservative estimate compared to the results of Kuo et al. (2004), who found the observation error of refractivity to be of the order of 0.3–0.5 % at 5–25 km.

As a further result, refractivity error correlation functions are displayed in Fig. 4 for three different heights, ~10 km, ~20 km, ~30 km, representative for troposphere, lower and upper stratosphere. Basically, these functions express the correlation of errors at these heights with the errors in the remainder of the profile. The ECMWF refractivity error correlation functions (dotted) show negative correlation features in the vicinity of the peaks whilst the correlation functions for the combined error (solid with diamond shaped symbols) show a flattening. These features suggest that the correlation wings are dominated by the observed data.

For the construction of refractivity observation error covariance matrices for data assimilation systems we therefore suggest a combination of the observed Rel.StdDev with the total error correlation matrix. We provide simple analytical formulations of refractivity error covariance matrices, which were deduced in a simulation study for a Metop/GRAS receiving system (Steiner and Kirchengast 2005). The functional formulations for Rel.StdDev and for correlation functions depend on a few parameters, which can be fitted for any given data set. Table 2 summarizes the functions. Using them for Rel.StdDev and approximating an exponential drop-off for the error correlations, a simple covariance matrix model $\boldsymbol{S}$ for the observed refractivity error can then be constructed via

$$\boldsymbol{S} = s_i s_j \exp\left[-\left|z_i - z_j\right| / L(z)\right]. \tag{5}$$

Table 2. Rel.StdDev $s(z)$ model for CHAMP refractivity with respective fitting parameters: z_{troptop} denoting the top level of the “troposphere domain”, z_{stratbot} the bottom level of the “stratosphere domain”, s_{utls} the Rel.StdDev between z_{troptop} and z_{stratbot}, s_0 the Rel.StdDev at ~1 km, H_{strat} the scale height of error, and $L(z)$ the correlation length, respectively.

<table>
<tr><th></th><th colspan="2">Relative Standard Deviation $s(z)$</th><th>Correlation Length $L(z)$</th></tr>
<tr><td>$2\text{ km} < z \le z_{\text{troptop}}$</td><td>$s_{\text{utls}}+s_0\,[1\text{km}/z - 1\text{km}/z_{\text{troptop}}]$</td><td rowspan="3">$s_{\text{utls}} = 0.5$ %
$s_0 = 4.5$ %
$z_{\text{troptop}} = 14$ km
global/NH: $z_{\text{stratbot}} = 20$ km
SH: $z_{\text{stratbot}} = 18$ km
global/SH: $H_{\text{strat}} = 15$ km
NH: $H_{\text{strat}} = 30$ km</td><td>$L = 2$ km</td></tr>
<tr><td>$z_{\text{troptop}} < z < z_{\text{stratbot}}$</td><td>$s_{\text{utls}}$</td><td rowspan="2">linear decrease to $L = 1$ km at z=50 km</td></tr>
<tr><td>$z_{\text{stratbot}} \le z < 35\text{ km}$</td><td>$s_{\text{utls}} \exp[(z - z_{\text{stratbot}})/H_{\text{strat}}]$</td></tr>
</table>

Figure 3 visualizes the analytical functions (thin solid) for the observed Rel.StdDev (thick solid) for the JJA 2003 season. In order to fit the seasonal behavior we adjusted the scale height of error H_{strat} to 30 km for summer (NH) and the bottom level of the stratosphere domain z_{stratbot} to 18 km for winter (SH). The validity of the fit regarding the upper height limit depends on the receiving system, e.g., 35 km for CHAMP data and near 50 km for Metop/GRAS (Steiner and Kirchengast 2005).

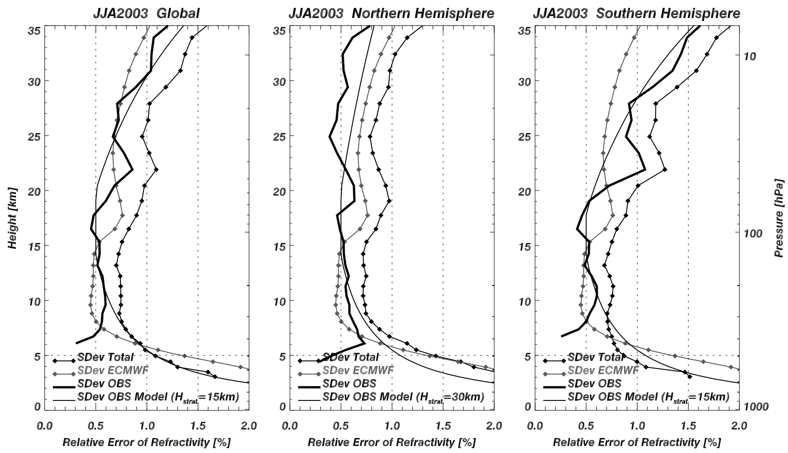

Fig. 3. Rel.StDev of refractivity for JJA 2003: combined (black diamond shaped symbols), ECMWF (gray diamond shaped symbols), observed (black thick), model (black thin); global (left), NH (middle), SH (right).

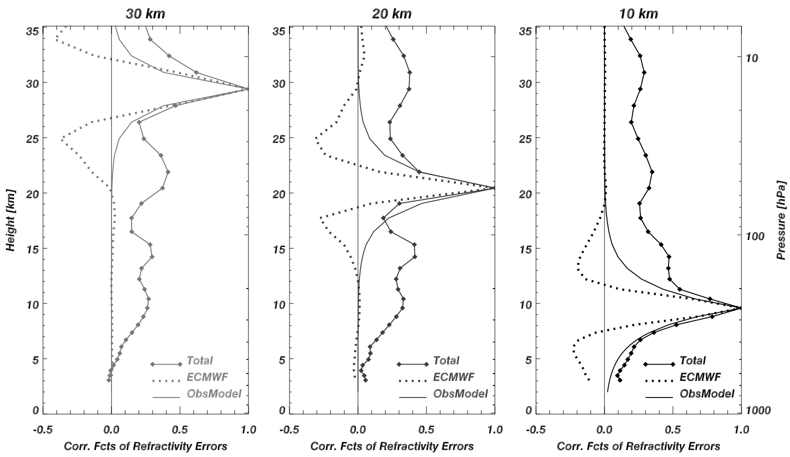

Fig. 4. Error correlation functions for the refractivity error: combined (solid line with diamond shaped symbols), ECMWF (dotted), and model (solid) shown for three heights ~30 km (light gray), ~20 km (gray), ~10 km (black).

6 Summary and Conclusions

As a follow-on study to the ensemble-based error analysis of simulated RO data (Steiner and Kirchengast 2004, 2005) we performed an error analysis for CHAMP RO refractivity profiles, processed with the IGAM CCRv2 scheme, for two seasons, DJF 2002/03 and JJA 2003. The error statistics was based on a comparison to reference profiles from ECMWF analyses fields, implying that the statistics includes both, the observation error and the ECMWF model error. In order to separate the errors, we performed an error estimation of the ECMWF error based on error propagation of temperature, humidity, and pressure error into refractivity error. Finally, the subtraction of the ECMWF error from the combined error allowed an estimation of the global observation error.

The relative refractivity bias of CHAMP RO with respect to ECMWF was found to, in general, oscillate around –0.4 % at 5–25 km globally. Wavelike structures apparent in SH winter at high latitudes are an indication that the ECMWF fields do not accurately represent the polar vortex (Gobiet et al. 2005). The smallest bias occurs at NH high latitudes in JJA. The combined Rel.StdDev of refractivity was found to be 0.7–1 % at 5–25 km height showing larger values in winter than in summer in the upper stratosphere at mid- and high latitudes. The estimated ECMWF refractivity error (2xT case) was found to be 0.5–0.75 % at 8–30 km. The global observation error of CHAMP refractivity was found to be 0.5 % at 6–18 km increasing to 1 % at 30 km globally, for mid- and high latitudes being ~0.5 % throughout this height range. These estimates are slightly more conservative than the 0.3–0.5 % results of Kuo et al. (2004).

In addition we analyzed refractivity error correlations. The ECMWF refractivity error correlation functions show negative correlation features in the vicinity of the peaks whilst the correlation functions for the combined error show a flattening. These features suggest that the correlation wings are dominated by the observed data. We therefore suggest a combination of the observed Rel.StdDev with the total error correlation matrix for the construction of observation error covariance matrices for data assimilation systems. These observation error covariance matrices can be approximated with simple analytical functions presented in Steiner and Kirchengast (2005); we presented parameters adjusted to the CHAMP CCRv2 performance. The refractivity error covariance formulation provided may be useful for implementation in optimal estimation parts of retrieval algorithms as well as in data assimilation systems.

Acknowledgments. The authors gratefully acknowledge the GFZ Potsdam, Germany, for the provision of CHAMP data; T. Schmidt for providing technical support and J. Wickert for scientific discussion. M. Borsche (WegCenter, Univ of Graz, Austria) is thanked for the processing of the CHAMP data sets and M. Fisher (ECMWF, Reading, UK) for providing error specifications for ECMWF analyses. The authors are thankful for valuable discussions on the topic with A. Gobiet (WegCenter, Univ of Graz, Austria), X.-Y. Huang (UCAR, Boulder, CO, USA), and C. Marquardt (EUMETSAT, Darmstadt, Germany). A.K.S. was funded from the START research award of G.K. financed by the Austrian Ministry for Education, Science, and Culture under Program Y103-N03 of the Austrian Science Fund.

References

Borsche M, Gobiet A, Steiner AK, Foelsche U, Kirchengast G, Schmidt T, Wickert J (2006) Pre-operational retrieval of radio occultation based climatologies. This issue

Foelsche U, Kirchengast G (2004) Sensitivity of GNSS occultation profiles to horizontal variability in the troposphere: A simulation study. In: Kirchengast G, Foelsche U, Steiner AK (eds) Occultations for Probing Atmosphere and Climate. Springer-Verlag, Berlin Heidelberg, pp 127–136

Gobiet A, Kirchengast G (2004a) Advancement of GNSS radio occultation retrieval in the upper stratosphere. In Kirchengast G, Foelsche U, Steiner AK (eds) Occultations for Probing Atmosphere and Climate. Springer-Verlag, Berlin Heidelberg, pp 137–148

Gobiet A, Kirchengast G (2004b) Advancements of GNSS radio occultation retrieval in the upper stratosphere for optimal climate monitoring utility. J Geophys Res 109(D24110), doi:10.1029/2004JD005117

Gobiet A, Foelsche U, Steiner AK, Borsche M, Kirchengast G, Wickert J (2005) Climatological validation of stratospheric temperatures in ECMWF operational analyses with CHAMP radio occultation data. Geophys Res Lett 32(L12806), doi:10.1029/2005GL022617

Healy SB, Jupp AM, Marquardt C (2005) Forecast impact experiment with GPS radio occultation measurements, Geophys Res Lett 32:L03804, doi:10.1029/2004GL020806

Hollingsworth A, Lönnberg P (1986) The statistical structure of short range forecast errors as determined from radiosonde data. Part I: The wind field. Tellus 38A:111–136

Kuo Y-H, Sokolovskiy SV, Anthes RA, Vandenberghe F (2000) Assimilation of GPS radio occultation data for numerical weather prediction. Terr Atmos Oceanic Sci 11:157–186

Kuo Y-H, Wee T-K, Sokolovskiy S, Rocken C, Schreiner W, Hunt D, Anthes RA (2004) Inversion and error estimation of GPS radio occultation data. J Meteorol Soc Japan 82: 507–531

Smith EK, Weintraub S (1953) The constants in the equation for atmospheric refractive index at radio frequencies. Proc of the IRE 41:1035–1037

Steiner AK, Kirchengast G (2004) Ensemble-based analysis of errors in atmospheric profiles retrieved from GNSS occultation data. In: Kirchengast G, Foelsche U, Steiner AK (eds) Occultations for Probing Atmosphere and Climate. Springer-Verlag, Berlin Heidelberg, pp 149–160

Steiner AK, Gobiet A, Foelsche U, Kirchengast G (2004) Radio occultation data processing advancements for optimizing climate utility. IGAM/Uni Graz Tech Rep for ASA No 3/2004

Steiner AK, Kirchengast G (2005) Error analysis for GNSS radio occultation data based on ensembles of profiles from end-to-end simulations. J Geophys Res 110(D15307), doi:10.1029/2004JD005251

Syndergaard S, Flittner DE, Kursinski ER, Feng DD, Herman BM, Ward DM (2004) Simulating the influence of horizontal gradients on retrieved profiles from ATOMS occultation measurements – a promising approach for data assimilation. In: Kirchengast G, Foelsche U, Steiner AK (eds) Occultations for Probing Atmosphere and Climate. Springer-Verlag, Berlin Heidelberg, pp 221–232

Syndergaard S, Kuo Y-H, Lohmann M (2006) Observation operators for the assimilation of occultation data into atmospheric models: A review. This issue